Modulation of π-Electron Conjugation in Oligo(triacetylene) Chromophores by Incorporation of a Central Spacer

by **Rainer E. Martin**, **Jennifer A. Wytko**, and **François Diederich***

Laboratorium für Organische Chemie, ETH-Zentrum, Universitätstrasse 16, CH-8092 Zürich

and **Corinne Boudon**, **Jean-Paul Gisselbrecht**, and **Maurice Gross**

Laboratoire d'Electrochimie et de Chimie Physique du Corps Solide, Faculté de Chimie, Université Louis Pasteur and CNRS, UMR n° 7512, 4, rue Blaise Pascal, F-67000 Strasbourg

A comprehensive series of trimeric hybrid oligomers **4**–**14** (*Fig. 2*) was prepared by insertion of different hetero-spacers between two (*E*)-hex-3-ene-1,5-diyne (=(*E*)-1,2-diethynylethene, DEE) moieties, and the optical and electrochemical properties of the resulting π-conjugated materials compared to those of the DEE dimer **2** and trimer **3**, which formally contains a DEE moiety as homo-spacer. The hetero-spacers varied from benzenoid (phenylene, naphthalene, biphenylene, anthracene), to π-electron-deficient (pyrazine, pyridine) and π-electron-rich (thiophene, furan) aromatic rings, and to an organometallic *trans*-Pt(PEt_3)$_2$ fragment. The hybrid oligomers were synthesized following a general strategy which relied on the *Sonogashira* cross-coupling between mono-deprotected DEE **15** and the appropriately bis-functionalized spacer (*Scheme* and *Table 1*). UV/VIS Studies revealed that the majority of the hetero-spacers were less effective than the homo-spacer DEE in facilitating π-electron delocalization along the linearly conjugated oligomeric backbone (*Table 2* and *Fig. 3*). With increasing degree of benzenoid aromaticity in the hetero-spacer, the electronic communication between the terminal DEE moieties in the hybrid oligomers was reduced. As a remarkable exception, a large bathochromic shift of the longest-wavelength absorption maximum, which is indicative of enhanced π-electron delocalization, was obtained upon introducing an anthracene-9,10-diyl moiety as hetero-spacer into oligomer **7** (*Figs. 3* and *6*). Electrochemical investigations by cyclic and steady-state voltammetry confirmed the limited extent of π-electron delocalization in the majority of the hybrid oligomers (*Table 3*). The fluorescence properties of many of the DEE hybrid materials were dramatically enhanced upon incorporation of the hetero-spacers (*Table 2*). The heterocyclic derivatives **10**–**12**, containing pyridine, pyrazine, or thiophene spacers, respectively, displayed a strong fluorescence emission, which is present to a significant extent neither in DEE homo-oligomers nor in the individual heteroaromatic spacer components, demonstrating the value of combining different repeat units to modulate oligomeric and polymeric properties. The pyridine derivative **10** provided an interesting example of a molecular system, in which both the electronic absorption (*Fig. 4*) and emission characteristics (*Table 2*) can be reversibly switched as a function of pH (*Fig. 5*).

1. Introduction. – In recent years, π-conjugated organic compounds have become a widely investigated class of advanced materials as they exhibit a variety of interesting electronic and photonic properties. One of the most attractive characteristics of organic materials is the amenability to optimize their physical properties by rational modification of their molecular structures. A further advantage of organic materials, compared to the classical inorganic counterparts, arises from the generally simple ways they can be processed, for instance by inexpensive spin coating or casting from solution. Recent developments in both low-molecular-weight π-conjugated chromophores and polymers have led to their use in practical devices exploiting effects ranging from magnetism [1], conductivity [2], electronically stimulated light emission (LEDs) [3],

and field-effect charge mobility (field-effect transistors, FETs) [4] to nonlinear optical responses [5].

Recently, we have already reported the synthesis of two series **1a** and **1b** (*Fig. 1*) of highly soluble monodisperse oligomers containing (*E*)-hex-3-ene-1,5-diyne (=(*E*)-1,2-diethynylethene, DEE) repeating units [6–8]. These oligomers served as invaluable model compounds for high-molecular-weight poly(triacetylene) (PTA) polymers [9][10] and allowed the establishment of comprehensive structure-property relationships for redox as well as linear and nonlinear optical properties. PTA Polymers [9], their monomeric components, such as arylated DEEs and tetraethynylethenes (= 3,4-diethynylhex-3-ene-1,5-diynes, TEEs) [11], and linear [11] and cyclic [12] oligomers made of arylated DEEs and TEEs feature attractive nonlinear optical (NLO) properties combined with good solution processability and thermal stabilities.

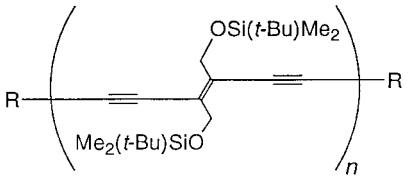

1a R = $SiMe_3$ n = 1–6

1b R = $SiEt_3$ n = 1,2,4,6,8,12,16

Fig. 1. *Two series of monodisperse poly(triacetylene) PTA oligomers*

Our research on novel acetylenic materials now targets the combination of DEE moieties with other interesting π-conjugated modular building blocks with the aim to construct hybrid materials with further enhanced NLO responses or luminescence properties. While DEE oligomers such as those in the series **1a** and **1b** display increasing third-order optical nonlinearities with increasing chain-length [6], they exhibit only little fluorescence emission. The introduction of aromatic spacers between two DEE moieties may alter both linear and nonlinear optical as well as fluorescence properties, thus opening the way to new and interesting classes of oligomers and polymers.

The spacers for insertion into the dimeric DEE **2**, giving access to the hybrid chromophores **3**–**14** (*Fig. 2*), were selected to cover a wide range of electronic properties. Although organic NLO materials usually have a much higher NLO response than inorganic materials, their optical application is often limited by the strong, conjugation-induced red-shifts of their longest-wavelength electronic absorption bands from the UV to the visible region [13]. *Zyss* [14], and *Moylan et al.* [15] have indicated that partial interruption of chain conjugation in linearly π-conjugated materials, for instance, by incorporation of an appropriate spacer, might lead to good NLO properties and avoid extension of the electronic absorptions into the visible region. Thus, benzenoid hetero-spacers[1]) were incorporated into the hybrid oligomers **4**–**9** in an attempt to reduce the efficiency of the overall linear π-electron

[1]) We define as homo-spacer a DEE moiety which is inserted between other DEE units as in **3**. Hetero-spacers are all the other spacers in the hybrid oligomers **4**–**14**.

delocalization through competition with localized benzenoid π-electron conjugation, thereby shifting the electronic end absorptions to higher energy. On the other hand, we hoped that the strong fluorescence emission, which is characteristic of naphthalene and anthracene chromophores, would be maintained in the hybrid oligomers **6** and **7**. In compounds **10**–**13**, aromatic heterocycles, ranging from electron-deficient pyridine and pyrazine to electron-rich thiophene and furan, were inserted as hetero-spacers. Also, the *trans*-$Pt^{II}(PEt_3)_2$ center in **14** was expected to partially interrupt π-electron conjugation along the linear backbone [16]. For further comparison, the trimeric PTA oligomer **3** [6], with a DEE homo-spacer, was also considered in this study.

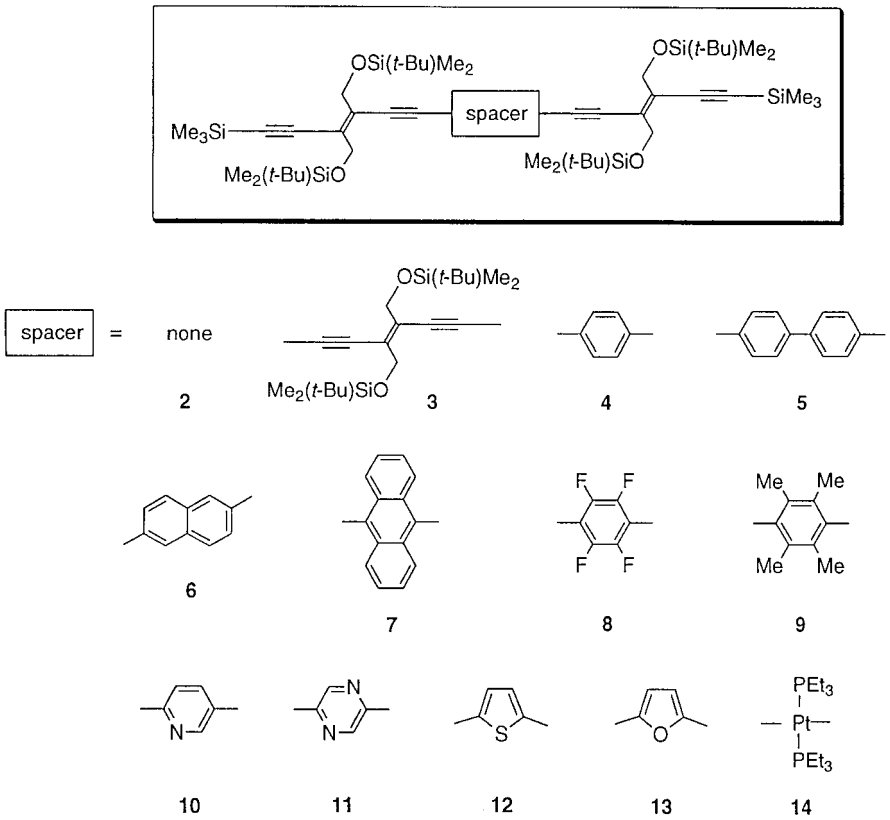

Fig. 2. *Hybrid materials obtained by insertion of functional π-conjugated spacers between two DEE moieties*

Here, we describe the synthesis of the new hybrid oligomers **4**–**14** (for a hybrid oligomer with a porphyrin 'hetero-spacer' inserted between two DEE moieties, see [17]) and report comprehensive investigations of their electronic properties as evaluated from UV/VIS, fluorescence, and electrochemical data (for a recent review on π-conjugated oligomers, see [18]). We show that the pyridine derivative **10** acts as a proton-switchable chromophore, which features a strong pH dependency of both its electronic absorption and emission properties. The nonlinear optical properties of the novel materials will be reported elsewhere.

2. Results and Discussion. – 2.1. *Synthesis.* Compounds **4**–**13** were prepared by *Sonogashira* cross-coupling [19] using 2 equiv. of mono-protected DEE **15** [10][20] and the appropriately bis-functionalized spacer in the presence of a Pd catalyst (*Scheme*). The detailed experimental conditions and product yields are given in *Table 1.* These reactions also afforded small quantities of **2** (typically around 5%) as a by-product owing to homo-coupling of **15**. Diiodinated spacers were chosen whenever possible, since [Pd]-mediated alkynylations of aryl iodides, compared to aryl bromides, are generally more efficient, and occur at lower temperatures [19]. All spacers were commercially available with the exception of 2,5-dibromopyrazine and naphthalene-2,6-diyl bis(trifluoromethanesulfonate), which were synthesized according to published procedures. The former was obtained in two steps by bromination of pyrazine-2-amine with *N*-bromosuccinimide (71%) [21] and subsequent diazotization of the NH_2 group (66%) [22]. The latter was prepared in 72% yield by esterification of naphthalene-2,6-diol with $(CF_3SO_2)_2O$ [23]. The cross-coupling of the electron-deficient pyridyl (**10**) and pyrazyl (**11**) derivatives proceeded – as expected [24] – in higher yields than the reaction of the electron-rich thiophene (**12**) or furan (**13**) spacers. A particularly low yield (12%) was obtained in the conversion of 1,4-diiodo-2,3,5,6-tetramethylbenzene to **9**, probably due to both steric hindrance and the electron-rich character of the spacer. The very low yield (7%) of the anthracene-bridged DEE **7** resulted from problems encountered during purification as well as from the low reactivity of the electron-rich dibromo spacer. A particularly efficient cross-coupling reaction was observed with naphthalene-2,6-diyl bis(trifluoromethanesulfonate) providing **6** in 84% yield [25].

The *trans*-Pt^{II} derivative **14** was prepared diastereoselectively in 65% yield by reacting **15** (2 equivs.) with *trans*-$[PtCl_2(PEt_3)_2]$ in THF in the presence of CuI catalyst and $(i\text{-}Pr)_2NH$ as base [26]. The mononuclear complex **14** displayed in the ^{1}H-NMR spectrum (200 MHz, $CDCl_3$) at 1.09 ppm a characteristic, *quintuplet*-type *multiplet* of higher order for the Me protons of the Et_3P groups, which couple to the adjacent CH_2 protons, the P-atoms, and the Pt-center [27]. The *trans*-geometry of the Et_3P groups at the Pt-center was indicated by the ^{31}P-NMR spectrum (121.5 MHz, $CDCl_3$), which featured a *triplet* at 12.41 ppm with a large coupling constant $J(^{31}P,^{195}Pt) = 2936$ Hz. Furthermore, the spectroscopic data of an analogous *trans*-$Pt^{II}(PEt)_3$ complex with two ligating TEE chromophores, the structure of which was elucidated by X-ray crystal-

Scheme. *Preparation of Compounds* **4**–**14**. Detailed reaction conditions and yields are listed in *Table 1.*

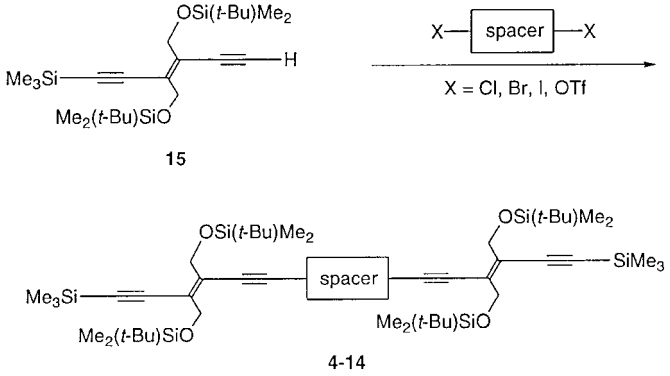

Table 1. *Reaction Conditions for the Cross-Coupling of DEE* **15** *with the Bis-functionalized Chromophores* X-Spacer-X *Affording the Hybrid Oligomers* **4**–**14**

Compound	X-Spacer-X [a])	Reaction Conditions [b])	Yield [%]
4	1,4-Diiodobenzene	Et_3N, CH_2Cl_2, r.t., 18 h	74
5	4,4′-Diiodobiphenyl	Et_3N, r.t., 18 h	48
6	Naphthalene-2,6-diyl bis(trifluoromethanesulfonate) [c])	$[Pd(PPh_3)_4]$, $(i\text{-}Pr)_2NH$, PhMe, 60°, 4 h	84
7	9,10-Dibromoanthracene	Et_3N, CH_2Cl_2, reflux, 36 h	7
8	1,4-Diiodo-2,3,5,6-tetrafluorobenzene	Et_3N, r.t., 22 h	33
9	1,4-Diiodo-2,3,5,6-tetramethylbenzene	Et_3N, PhMe, 70°, 18 h	12
10	2,5-Dibromopyridine	Et_3N, 80°, 18 h	71
11	2,5-Dibromopyrazine [d])	Et_3N, PhMe, 80°, 18 h	82
12	2,5-Diiodothiophene	Et_3N, PhMe, 60°, 18 h	52
13	2,5-Dibromofuran	Et_3N, PhMe, 70°, 48 h	30
14	*trans*-$[PtCl_2(PEt_3)_2]$	no Pd catalyst, CuI, $(i\text{-}Pr)_2NH$, THF, r.t., 20 h	65

[a]) 0.5 Equiv. were used. [b]) $[PdCl_2(PPh_3)_2]$ (3 mol-%) and CuI (6 mol-%) were employed as catalysts under an inert atmosphere for all coupling reactions unless indicated otherwise. [c]) Prepared according to [23]. [d]) Prepared according to [21] and [22].

structure analysis, provide additional support for the exclusive formation of *trans*-ligated **14** [28].

All new hybrid oligomers **4**–**14** are stable towards exposure to light and air under standard laboratory conditions and were fully characterized. Whereas the furan derivative **13** was isolated as oil, all other hybrid materials were crystalline solids which melted without decomposition.

2.2. *UV/VIS Studies.* The electronic absorption spectra of the DEE oligomers **2** and **3** and the hybrid materials **4**–**14** were measured in $CHCl_3$ at r.t. The longest-wavelength absorption maxima λ_{max}, which correlate with the extent of π-electron conjugation along the linear backbone, are listed in *Table 2*.

The insertion of a DEE moiety (a homo-spacer) into DEE dimer **2** under formation of trimer **3** generates a large bathochromic shift of the longest-wavelength absorption maximum from $\lambda_{max} = 376$ (**2**) to 407 (**3**) nm (*Fig. 3,a*) [6], in agreement with a significant increase in π-electron delocalization along the elongated backbone. In contrast, the insertion of a hetero-spacer between two DEE moieties, in most cases, did not produce a similar extension of π-electron conjugation (*Table 2*). Thus, the introduction of a phenylene (**4**) or naphthalene (**6**) spacer between two DEE moieties led to a near doubling of the molar extinction coefficients of the two longest-wavelength absorption bands as compared to DEE dimer **2** (*Fig. 3,b*). The maxima of these bands, as well as the spectral end-absorptions, however, appeared at nearly identical wavelengths in all three compounds. Similar spectral characteristics are observed for the other hybrid oligomers with phenylene (**8** and **9**), or biphenylene (**5**) spacers. Clearly, the benzenoid hetero-spacers are less effective than the central homo-spacer in DEE trimer **3** in transmitting π-electron delocalization along the oligomeric backbone.

On the other hand, introduction of the anthracene spacer in **7** produced a remarkable red-shift of all bands in the UV/VIS spectrum (*Fig. 3,b*), and the longest-wavelength absorption maximum appeared at $\lambda_{max} = 495$ nm. The overall shape of the

Table 2. *UV/VIS and Fluorescence Data of DEE Derivatives* **2**, **3**, *and Hybrid Oligomers* **4**–**14** *in* $CHCl_3$ *at Room Temperature*

Compound	λ_{max}/nm [a]) (ε/M^{-1} cm^{-1}) [e])	λ_{exc}/nm [b]) (ε/M^{-1} cm^{-1}) [e])	λ_{em}/nm [c])	Φ_F [d])
2	376 (24700) [f])	356 (25300)	425	0.01
3	407 (sh, 36700) [f])	356 (31800)	399, 440	0.01
4	374 (sh, 36700)	356 (52100)	394, 418	0.49
5	351 (76300)	356 (74600)	399, 421	0.73
6	381 (sh, 47500)	356 (58900)	398, 422	0.65
7	495 (42300)	336 (30500) [g])	508, 542	0.57
8	382 (57400)	356 (66600)	403, 425	0.46
9	384 (40100)	356 (46500)	403, 424	0.57
10	376 (sh, 10200)	356 (15400)	407, 421	0.40
10•**H**$^+$ [h])	380 (45300)	356 (35200)	480	0.07 [i])
11	392 (sh, 41900)	356 (39800)	427	0.65
11•**H**$^+$ [j])	382 (46500)	356 (33200)	427	0.03 [i])
12	404 (sh, 32400)	356 (32400)	430, 454	0.21
13	398 (sh, 23900)	356 (26300)	422	0.02
14	342 (42300)	356 (33000)	–	–

[a]) Experimentally observed longest-wavelength absorption maxima. [b]) Excitation wavelength. [c]) Fluorescence emission band. [d]) Fluorescence quantum yield; anthracene ($\Phi_F = 0.33$) and quinine sulfate ($\Phi_F = 0.55$) were used as reference compounds [29]. [e]) Molar extinction coefficient. [f]) Values taken from [6]. [g]) Only weak absorptivity at the excitation wavelength (356 nm) used for the other oligomers. [h]) HCl was used as proton source. [i]) Fluorescence quantum yields decreased with increasing acid concentration. [j]) CF_3COOH was used as proton source.

spectrum is more characteristic of an anthracene than an oligomeric DEE chromophore; however, the two transitions with maxima at 495 and 335 nm are bathochromically shifted by nearly 100 nm compared to the two longest-wavelength absorptions of the pure aromatic hydrocarbon [30].

Insertion of the Pt^{II}-center in **14** reduces the π-electron delocalization along the linear backbone as compared to the DEE dimer **2**. This is indicated by a significant blue shift of the longest-wavelength absorption maximum (*Table 2*). *Ziessel* and co-workers also noted the insulating effect of Pt^{II} in *trans*-bis(σ-acetylide) complexes [31]; on the other hand, *Faust et al.* had provided evidence for some degree of electronic communication across the Pt^{II}-center in such complexes, presumably mediated by metal-to-ligand charge transfer (MLCT) [16]. A comparison of UV/VIS data indeed shows that the two terminal DEE chromophores in **14** are not fully insulated by the metal center: bis-silyl-protected monomeric DEE (=(*E*)-3,4-bis{[(*tert*-butyl)dimethylsilyloxy]methyl}-1,6-bis(trimethylsilyl)hex-3-ene-1,5-diyne) features its longest-wavelength absorption maximum at $\lambda_{max} = 296$ nm [6], whereas this band in **14** appears at $\lambda_{max} = 342$ nm (*Table 2*).

A more efficient π-electron delocalization along the oligomeric backbone is obtained upon introduction of electron-rich heterocyclic spacers. The longest-wavelength absorption maxima of thiophene derivative **12** ($\lambda_{max} = 404$ nm, sh) and furan derivative **13** ($\lambda_{max} = 398$ nm, sh) (*Fig. 3,c*) show significant bathochromic shifts when compared to DEE dimer **2** (*Fig. 3,a*) or the oligomers with phenylene spacers (*Fig. 3,b*). This can be explained by both the reduced benzenoid aromaticity of these

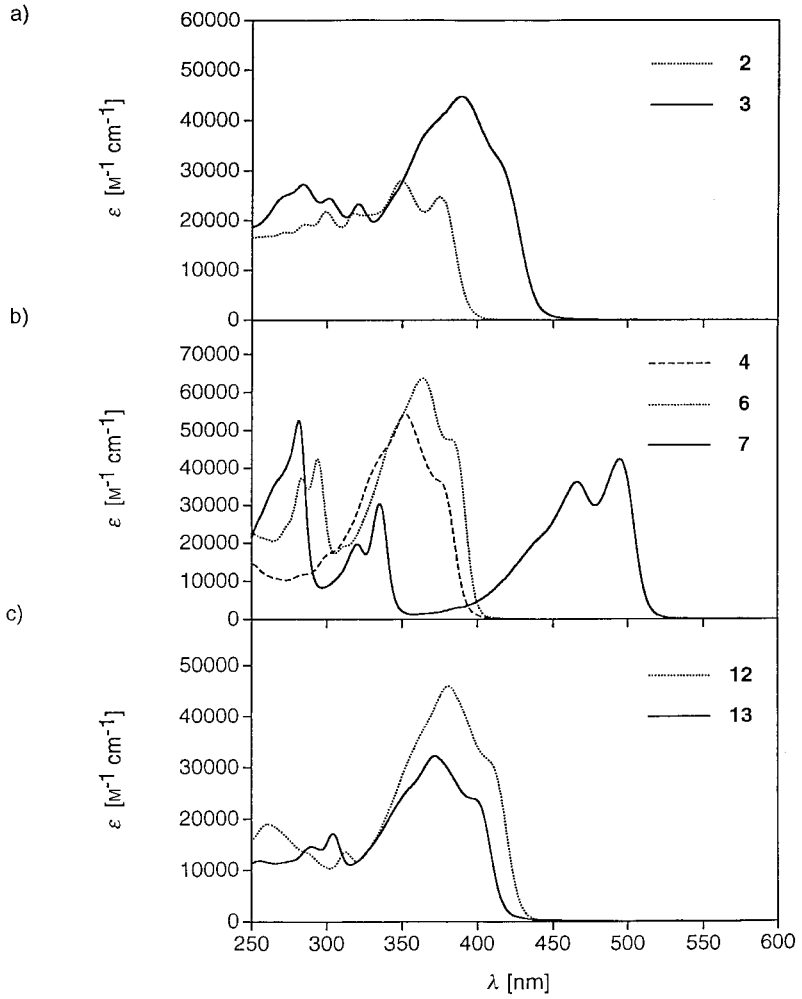

Fig. 3. *Comparison of electronic absorption spectra in $CHCl_3$. a*) DEE Dimer **2** and trimer **3**. *b*) Hybrid oligomers with phenylene (**4**), naphthalene (**6**), and anthracene (**7**) spacers. *c*) Hybrid oligomers **12** and **13**, incorporating thiophene and furan spacers, respectively.

hetero-spacers and their electron-rich character, which may induce intramolecular donor-acceptor interactions with the strongly electron-attracting DEE moieties [17]. Such interactions, however, are not solely responsible for the observed absorption behavior, since thiophene, with lower electron excessivity than furan [32], produces a slightly greater red shift.

Insertion of the N-containing heterocycles pyridine (in **10**) and pyrazine (in **11**) produced several interesting effects. Whereas the pyridine spacer did not shift the longest-wavelength absorption maximum (sh at $\lambda_{max} = 376$ nm), compared to DEE dimer **2**, insertion of pyrazine caused a substantial bathochromic shift to $\lambda_{max} = 392$ nm (sh, *Fig. 4,a*). This difference can tentatively be explained by the difference in the

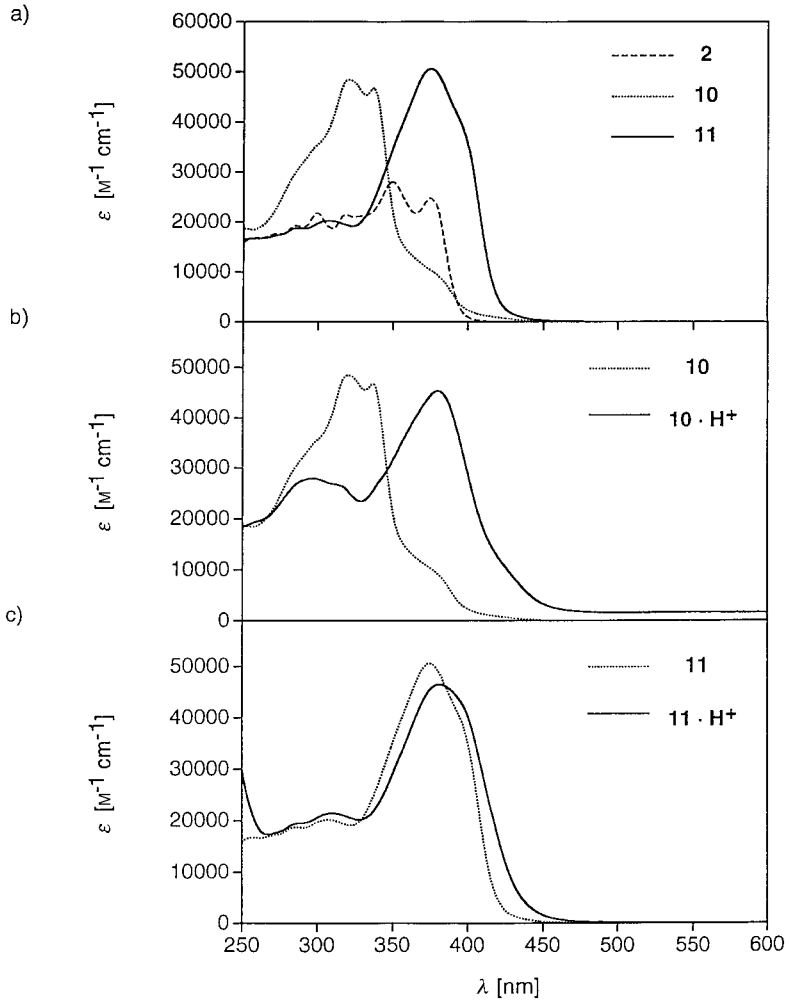

Fig. 4. *Comparison of electronic absorption spectra in $CHCl_3$. a*) DEE Dimer **2** and hybrid oligomers **10**, with a pyridine, and **11**, with a pyrazine spacer. *b*) Pyridine derivative **10** before and after protonation with HCl. *c*) Pyrazine derivative **11** before and after protonation with CF_3COOH.

benzenoid aromaticity of the two spacers, which is more pronounced in pyridine than in pyrazine [33].

The effects of protonation with conc. aq. HCl or conc. CF_3COOH on the UV/VIS spectral properties of **10** and **11** again differed substantially. Whereas protonation of the pyridine derivative **10** caused a large bathochromic shift ($\Delta\lambda = 43$ nm, *Fig. 4,b*) of the most intense absorption band, the corresponding band in the spectrum of **11** was much less affected by protonation ($\Delta\lambda = 10$ nm, *Fig. 4,c*). These shifts were fully reversible and, upon treatment with base, the original spectra of the unprotonated species were recovered. Although *N*-protonation involves an orbital orthogonal to those participating in the linear π-electron conjugation along the oligomeric backbone,

it facilitates the latter conjugation strongly, in particular in the pyridine derivative. We propose that the introduction of the charges reduces the local benzenoid aromaticity which, in turn, favors extended π-conjugation. Reversibly proton-switchable chromophores such as **10** [34] (for some recent literature concerning molecular switches, see [35]) hold promise to fulfill a wide variety of functions ranging from proton sensors to pH-controllable materials for electroluminescent [36] and linear or nonlinear optical applications.

2.3. *Fluorescence Studies.* The majority of the hybrid oligomers displayed a strong fluorescence with a high quantum yield Φ_F in $CHCl_3$ at room temperature (*Table 2*). Since the dimeric and trimeric DEE oligomers **2** and **3** showed only a very weak emission efficiency ($\Phi_F = 0.01$), this increase in fluorescence quantum yield must be attributed largely to the insertion of the hetero-spacers. Among the oligomers with aromatic hydrocarbon spacers, the biphenyl derivative **5** ($\Phi_F = 0.73$) displayed the highest fluorescence quantum yield, followed by the naphthalene derivative **6** ($\Phi_F = 0.65$).

Simple heterocycles such as pyridine, pyrazine, or thiophene in general do not exhibit a significant fluorescence emission [37]. Upon introduction of these compounds as spacers between two DEE moieties, however, the resulting hybrid oligomers **10**–**12** displayed a strong luminescence with high quantum yields. Protonation of the N-heterocyclic derivatives **10** and **11** resulted in nearly complete quenching of the fluorescence; quantum yields decreased steadily with increasing amounts of acid. Since the initial luminescence emission was fully regained upon addition of base, compounds **10** and **11** feature reversible proton-controlled switching of both their electronic absorption and emission characteristics (*Fig. 5*). Interestingly, protonation of the pyridine spacer in **10** caused a bathochromic shift of $\Delta\lambda_{em} = 59$ nm in the emission maximum from $\lambda_{em} = 421$ nm to $\lambda_{em} = 480$ nm, whereas the emission maximum of the

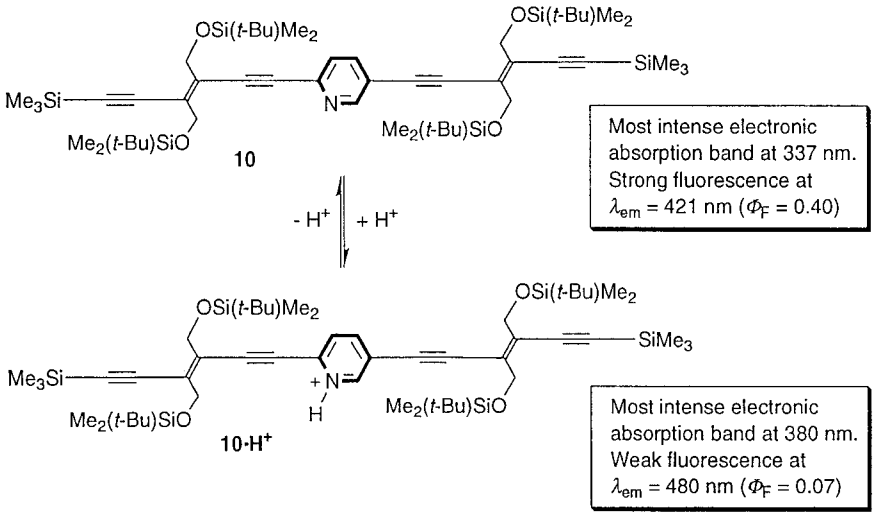

Fig. 5. *Reversible proton-driven switching of the electronic absorption and emission characteristics of hybrid oligomer* **10** *with a pyridine spacer*

pyrazine derivative **11** was, within the limits of uncertainty, unaffected by protonation (*Table 2*). This result is in agreement with the larger protonation-induced bathochromic shift measured for the electronic absorption bands of **10**, as compared to **11** (*Sect. 2.2*).

2.4. *Electrochemical Investigations.* The redox characteristics were investigated by cyclic (CV) and steady-state voltammetry (SSV) in CH_2Cl_2 (+ 0.1M Bu_4NPF_6), and the results are summarized in *Table 3*. As a general trend, it was found that the redox properties of the hybrid oligomers resemble those of the DEE oligomers **2** and **3**, featuring one, mostly reversible one-electron reduction and one, often irreversible, one-electron oxidation step. Irreversible reduction signals result mainly from the potentials being similar to the solvent discharge. The majority of the hybrid oligomers is reduced at more negative potentials than the DEE dimer **2**. Only for the derivatives containing anthracene (**7**), 2,3,5,6-tetrafluorobenzene (**8**), and pyrazine (**11**) were the first reduction potentials less negative than that of DEE dimer **2**. These results suggest that, for the majority of hybrid oligomers investigated, there exists only weak π-electron delocalization along the conjugated backbone.

Table 3. *Cyclic and Steady-State Voltammetric Redox Characteristics of the DEE Oligomers* **2** *and* **3**, *and Hybrid Oligomers* **4**–**14**

Compound	Cyclic voltammetry			Steady-state voltammetry	
	E'° [a]) (ΔE_p/mV) [b])	E_{pc} [c])	E_{pa} [d])	$E^{red}_{1/2}$ [e]) (slope/mV) [f])	$E^{ox}_{1/2}$ [e]) (slope/mV) [f])
2 [g])	−2.10 (130) [h])	–	+1.29	−2.12 (70)	–
3 [g])	−1.88 (80)	−2.09	+1.25	–	–
4	–	−2.44	+1.24	−2.46 (150)	+1.24 (78) +1.42 (98)
5	–	−2.37 −2.45	+1.18	–	+1.17 (97)
6	–	−2.28 −2.38	+1.17	−2.28 (96) −2.44 (80)	+1.14 (75)
7	−1.72 (85) +0.72 (90)	−2.13	+1.22	−1.74 (80) −2.12 (90)	+0.72 (67) +1.22 (90)
8	−1.90 (130)	−2.23	–	−1.91 (65) −2.32 (65)	–
9	+1.02 (115)	−2.35	–	–	+1.01 (80)
10	–	−2.25 −2.43	+1.43	–	+1.44 (129)
11	−1.80 (105)	−2.20	–	−1.83 (113)	–
12	+1.04 (150) [i])	−2.16	–	−2.32 (200)	+1.02 (71) +1.37 (181)
13	+1.00 (130)	−2.40	–	−2.32 (123)	+1.00 (106)
14	+0.72 (75)	–	+1.16	–	+0.73 (68) +1.16 (85)

[a]) *V vs.* Fc/Fc$^+$, glassy C-electrode in CH_2Cl_2 + 0.1M Bu_4NPF_6, scan rate $\nu = 0.1$ V s^{-1}, formal redox potential $E'^{\circ} = (E_{pa} + E_{pc})/2$. [b]) $\Delta E = E_{pa} - E_{pc}$, where subscripts pa and pc refer to the conjugated oxidation and reduction peak, respectively. [c]) Peak potential E_{pc} for irreversible reduction. [d]) Peak potential E_{pa} for irreversible oxidation. [e]) *V vs.* Fc/Fc$^+$, rotating disk electrode in CH_2Cl_2 + 0.1M Bu_4NPF_6. [f]) Logarithmic analysis of the wave obtained by plotting *E vs.* $\log[I/I_{lim} - I)]$. [g]) Taken from [6]. [h]) Reversible electron transfer at scan rates $\nu > 0.5$ V s^{-1}. [i]) Reversible electron transfer at scan rates $\nu > 1$ V s^{-1}.

The differences between the electrochemically determined first oxidation and first reduction half-wave potentials are in good agreement with the HOMO-LUMO gaps observed by UV/VIS spectroscopy. For example, the phenylene derivative **4** revealed its most intense absorption band at $\lambda = 352$ nm ($E = 3.52$ eV), and for the anthracene chromophore **7** the longest-wavelength absorption band was detected at $\lambda_{max} = 495$ nm ($E_{max} = 2.50$ eV). This is in agreement with the observed potential differences of 3.68 and 2.44 eV, respectively, from cyclic voltammetry. Time-resolved spectroelectrochemical measurements were carried out for the anthracene derivative **7**. The UV/VIS spectra recorded during the oxidation process exhibited well-defined isosbestic points which confirm the interconversion of the two redox-stable states, namely the neutral initial species and the generated radical cation, on the time scale of the measurement (*Fig. 6*).

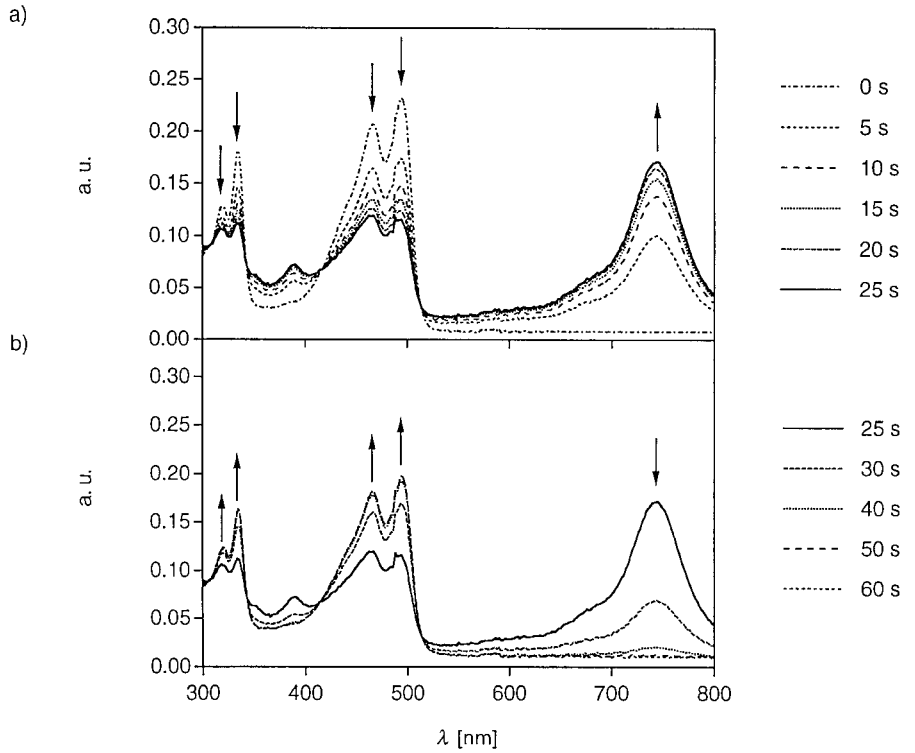

Fig. 6. *Time-resolved UV/VIS absorption spectra for* a) *oxidation and* b) *re-reduction of* **7** *in* CH_2Cl_2 (+ 0.1M Bu_4NPF_6)

The mononuclear Pt^{II} spacer complex **14** could be oxidized reversibly at $E'^{o}_{ox} = +0.72$ V by cyclic voltammetry at sweep rates higher than $\nu = 0.1$ V s^{-1}, whereas for lower sweep rates the oxidative electron-transfer step became irreversible. This redox behavior and the position of the oxidation potential are in agreement with the generation of an unstable Pt^{III} complex [38]. However, within the experimentally accessible potential range of cyclic and steady-state voltammetry, no reduction of compound **14** occurred.

3. Conclusions. – The aim of this study was to explore how the properties of oligomers made from (*E*)-1,2-diethynylethene (*DEE*) repeat units can be tuned or changed by the insertion of spacer chromophores. For this purpose, a series of eleven hybrid oligomers **4**–**14** was prepared in which mostly aromatic hetero-spacers with different electronic characteristics were introduced between the two DEE moieties. UV/VIS Studies revealed that, with a few exceptions, the hetero-spacers in **4**–**14** were less effective than the homo-spacer DEE in trimeric **3** in facilitating π-electron delocalization along the linear conjugated oligomeric backbone. The longest-wavelength absorption maxima λ_{max}, which were taken as experimental criteria for estimating the extent of π-electron delocalization in the hybrid oligomers, were shifted to higher energy (compared to DEE trimer **3**) when the spacer featured a high degree of localized benzenoid aromaticity. A truly remarkable bathochromic shift of λ_{max}, for which a good explanation will require theoretical calculations, was obtained only when an anthracene-9,10-diyl moiety was introduced as a spacer in oligomer **7**. Electrochemical investigations by CV and SSV confirmed the reduced capability of the various hetero-spacers in promoting π-electron delocalization along the oligomeric backbone.

On the other hand, fluorescence studies clearly demonstrated that a desirable function can be created or strongly enhanced upon insertion of hetero-spacers into pure DEE oligomers. Thus, the heterocyclic derivatives **10**–**12** containing pyridine, pyrazine, or thiophene spacers, respectively, feature a strong fluorescence emission which is present to a significant extent neither in DEE oligomers nor in the individual heteroaromatic spacer components. Furthermore, the pyridine derivative **10** provided a very good example of a molecular system in which *both* the electronic absorption and emission characteristics can be reversibly switched as a function of pH.

In the future, functions and processability of π-conjugated oligomers and polymers will increasingly be modulated and optimized by the incorporation of multiple different repeating units. Since an enormous number of compounds can potentially be prepared and screened for materials properties, solid-phase synthesis and combinatorial methods will undoubtedly be applied widely in the development and testing of innovative hybrid materials [18][39]. We are now focusing our research along these novel directions.

Experimental Part

General. Reagents and solvents were purchased reagent grade and used without further purification. Compounds **2**, **3** [6][8], **15** [10][20], naphthalene-2,7-diyl bis(trifluoromethanesulfonate) [23], and 2,5-dibromopyrazine [21][22] were prepared according to literature procedures. Anh. $MgSO_4$ was used as the drying agent after aqueous workup. Evaporation and concentration *in vacuo* were carried out at H_2O-aspirator pressure. All reactions were performed in standard glassware under an inert atmosphere of Ar. Careful degassing and a positive pressure of Ar during the reaction were essential to the success of [Pd]-catalyzed cross-couplings. Degassing of solvents was accomplished by vigorously bubbling Ar through the soln. for at least 45 min or by a minimum of three freeze-thaw-pump cycles. Column chromatography (CC): SiO_2-*60* (70–270 mesh, 50–200 μm) from *Macherey-Nagel*, SiO_2-*60* (70–230 mesh, 63–200 μm) from *Merck*, or SiO_2-*60* (230–400 mesh, 40–63 μm) from *Fluka*. Prep. thin-layer chromatography (TLC): glass sheets covered with silica gel *60* F_{254} from *Merck* or *Polygram SIL G/UV*$_{254}$ from *Macherey-Nagel*; visualization by UV light or anisaldehyde stain. M.p.: *Büchi SMP-20*, uncorrected. UV/VIS Spectra (λ_{max} [nm]: ε[M^{-1} cm^{-1}]): *Varian-Cary-5*, at r.t. Fluorescence spectra (λ_{em} [nm]): *SPEX-1680 Fluorolog 0.22m Double Spectrophotometer* at r.t. Quinine sulfate and anthracene were used as reference compounds in quantum-yield determinations. IR Spectra

[cm^{-1}]: *Perkin Elmer-1600-FTIR*. ^{1}H- and ^{13}C-NMR Spectra: *Bruker-AMX-500*, *Varian Gemini-200* and *300* at r.t. in $CDCl_3$; solvent peaks (7.24 ppm for ^{1}H and 77.0 ppm for ^{13}C) as internal reference. MS (*m/z* (%)): EI (70 eV): *VG-Tribrid* spectrometer; FAB: *VG-ZAB-2SEQ* instrument with a 3-nitrobenzyl-alcohol matrix. Elemental analyses were effected by the Mikrolabor at the Laboratorium für Organische Chemie, ETH-Zürich.

Electrochemical Measurements. The electrochemical measurements were carried out at $20 \pm 2°$ in CH_2Cl_2 containing 0.1M Bu_4NPF_6 in a classical three-electrode cell. The electrochemical cell was connected to a computerized multipurpose electrochemical device (*DACFAMOV*, *Microtec-CNRS*, Toulouse, France) interfaced with an *Apple II* microcomputer. The working electrode was a glassy C-disk electrode used either motionless for CV (10 mV s^{-1} to 10 V s^{-1}) or as a rotating-disk electrode. The auxiliary electrode was a Pt wire, and a Ag wire was used as a pseudo-reference electrode. Time-resolved UV/VIS absorption spectra for the first oxidation of **7** were recorded in a thin-layer cell through an optically transparent thin-layer electrode (OTTLE) made of a Pt minigrid (1000 mesh). The auxiliary electrode was a Pt wire, and the reference electrode was Ag/AgCl/KCl (sat.). The optical path in the cell was *ca.* 0.1 mm. The thin-layer cell was placed in a diode-array UV/VIS spectrophotometer (*HP 8452A*) with a resolution of 2 nm, which was connected to an electrochemical unit (*Bruker-Ifelec*) for control and measurement of the electrochemical parameters. All potentials are referenced to the ferrocene/ferricinium (Fc/Fc^+) couple that was used as an internal standard. The accessible range of potentials was +1.2 to −2.2 V *vs.* Fc/Fc^+ on a glassy C-electrode in CH_2Cl_2. CH_2Cl_2 (spectroscopic grade) was purchased from *Merck*, dried over molecular sieves (4 Å), and stored under Ar prior to use. Bu_4NPF_6 was purchased electrochemical grade from *Fluka* and used as received.

General Workup for [Pd]-Catalyzed Alkynylations. Unless otherwise noted, [Pd]-catalyzed coupling reactions were worked up as follows. After reacting the aryl halide with the terminal alkyne for the indicated time period, the solvent or solvent mixtures were removed *in vacuo*. The residue was dissolved in a minimal amount of CH_2Cl_2 and passed through a plug of silica gel (SiO_2-*60*, CH_2Cl_2). Evaporation *in vacuo* gave the crude reaction mixtures, which were then purified as described in the individual procedures.

*1,4-Bis[(*E*)-3,4-bis[[(*tert*-butyl)dimethylsilyloxy]methyl]-6-(trimethylsilyl)hex-3-ene-1,5-diynyl]benzene* (**4**). A degassed soln. of **15** (0.10 g, 0.23 mmol), 1,4-diiodobenzene (0.038 g, 0.11 mmol), $[PdCl_2(PPh_3)_2]$ (0.005 g, 0.007 mmol), and CuI (0.003 g, 0.014 mmol) in Et_3N (2 ml) and CH_2Cl_2 (10 ml) was stirred at r.t. under Ar for 18 h. Workup and purification by CC (SiO_2-*60*; hexane/PhMe 2:1) gave **4** (0.081 g, 74%). White solid. M.p. 59–60°. UV/VIS ($CHCl_3$): 303 (17300), 340 (sh, 45700), 352 (54400), 374 (sh, 36700). IR ($CHCl_3$): 3022, 2956, 2953, 2856, 2133, 1472, 1470, 1250, 1207, 1100, 844, 817. ^{1}H-NMR (200 MHz, $CDCl_3$): 0.10 (*s*, 24 H); 0.19 (*s*, 18 H); 0.91 (*s*, 36 H); 4.48 (*s*, 4 H); 4.52 (*s*, 4 H); 7.36 (*s*, 4 H). ^{13}C-NMR (50 MHz, $CDCl_3$): −5.76; −0.84; 17.76; 25.26; 63.25; 63.45; 88.02; 100.14; 101.22; 106.52; 122.62; 129.16; 129.89; 130.68. FAB-MS: 947.5 (29, MH^+), 889.5 (100, $[M - Me_3C]^+$). Anal. calc. for $C_{52}H_{90}O_4Si_6$ (947.81): C 65.90, H 9.57; found: C 65.67, H 9.69.

*4,4′-Bis[(*E*)-3,4-bis[[(*tert*-butyl)dimethylsilyloxy]methyl]-6-(trimethylsilyl)hex-3-ene-1,5-diynyl]-1,1′-biphenyl* (**5**). A degassed soln. of **15** (0.10 g, 0.23 mmol), 4,4′-diiodobiphenyl (0.047 g, 0.11 mmol, *ca.* 90% purity), $[PdCl_2(PPh_3)_2]$ (0.004 g, 0.005 mmol), and CuI (0.001 g, 0.006 mmol) in Et_3N (10 ml) was stirred at r.t. under Ar for 18 h. Workup and purification by CC (SiO_2-*60*; hexane/PhMe 3:1) afforded **5** (0.047 g, 48%). Colorless solid. M.p. 102–103°. UV/VIS ($CHCl_3$): 270 (18800), 317 (sh, 39100), 351 (76300). IR ($CHCl_3$): 3000, 2956, 2936, 2856, 2133, 1600, 1472, 1463, 1250, 1183, 1100, 1039, 1006, 933, 839. ^{1}H-NMR (200 MHz, $CDCl_3$): 0.115 (*s*, 12 H); 0.119 (*s*, 12 H); 0.20 (*s*, 18 H); 0.92 (*s*, 18 H); 0.93 (*s*, 18 H); 4.52 (*s*, 4 H); 4.54 (*s*, 4 H); 7.49 (*d*, $J = 8.3$, 4 H); 7.56 (*d*, $J = 8.3$, 4 H). ^{13}C-NMR (50 MHz, $CDCl_3$): −5.73; −0.81; 17.79; 25.29; 63.32; 63.48; 87.03; 100.37; 101.32; 106.27; 121.98; 126.24; 128.84; 130.08; 131.32; 139.57. FAB-MS: 1023.6 (32, MH^+), 965.3 (100, $[M - Me_3C]^+$). HR-FAB-MS: 1022.5754 (M^+; $^{12}C_{58}H_{94}O_4{}^{28}Si_6{}^+$; calc. 1022.5767). Anal. calc. for $C_{58}H_{94}O_4Si_6 \cdot 1/2\ H_2O$ (1032.91): C 67.44, H 9.27; found: C 67.45, H 9.36.

*2,6-Bis[(*E*)-3,4-bis[[(*tert*-butyl)dimethylsilyloxy]methyl]-6-(trimethylsilyl)hex-3-ene-1,5-diynyl]naphthalene* (**6**). A degassed soln. of **15** (0.10 g, 0.23 mmol), naphthalene-2,6-diyl bis(trifluoromethanesulfonate) (0.046 g, 0.11 mmol), and $[Pd(PPh_3)_4]$ (0.016 g, 0.014 mmol) in PhMe (3 ml) and $(i\text{-}Pr)_2NH$ (4 ml) was heated at 60° under Ar for 4 h. Workup and purification by CC (SiO_2-*60*; hexane/PhMe 4:1 → 2:1; gradient) afforded **6** (0.092 g, 84%). Yellow solid. M.p. 100–102°. UV/VIS ($CHCl_3$): 283 (37300), 294 (42500), 364 (63700), 381 (sh, 47500). IR ($CHCl_3$): 3011, 2956, 2856, 2133, 1600, 1472, 1250, 1100, 894, 844. ^{1}H-NMR (500 MHz, $CDCl_3$): 0.13 (*s*, 12 H); 0.14 (*s*, 12 H); 0.22 (*s*, 18 H); 0.93 (*s*, 18 H); 0.94 (*s*, 18 H); 4.55 (*s*, 4 H); 4.57 (*s*, 4 H); 7.48 (*dd*, $J = 8.4$, 1.4, 2 H); 7.73 (*d*, $J = 8.4$, 2 H); 7.90 (br. *s*, 2 H). ^{13}C-NMR (125.8 MHz, $CDCl_3$): −5.07; −5.05; −0.14; 18.44; 18.45; 25.95; 64.00; 64.14; 87.87; 101.42; 101.95; 107.11; 121.53; 127.93; 128.93; 129.71; 130.70; 131.08; 132.42. FAB-MS: 995.4 (28, M^+); 939.4 (100, $[M - Me_3C]^+$). Anal. calc. for $C_{56}H_{92}O_4Si_6$ (997.85): C 67.41, H 9.29; found: C 67.55, H 9.10.

*9,10-Bis[(*E*)-3,4-bis[[(*tert*-butyl)dimethylsilyloxy]methyl]-6-(trimethylsilyl)hex-3-ene-1,5-diynyl]anthracene* (**7**). A degassed soln. of **15** (0.10 g, 0.23 mmol), 9,10-dibromoanthracene (0.038 g, 0.11 mmol), $[PdCl_2(PPh_3)_2]$ (0.005 g, 0.007 mmol), and CuI (0.003 g, 0.014 mmol) in Et_3N (15 ml) and CH_2Cl_2 (5 ml) was heated at reflux under Ar for 36 h. Workup and purification by CC (SiO_2-*60*; hexane → hexane/PhMe 2 : 1; gradient), prep. TLC (SiO_2-*60*; hexane/PhMe 2 : 1), and recrystallization from hot i-PrOH yielded **7** (0.008 g, 7%). Orange needles. M.p. 178–179°. UV/VIS ($CHCl_3$): 281 (52700), 320 (19700), 335 (30500), 466 (36200), 495 (42300). IR ($CHCl_3$): 3022, 2955, 2856, 2133, 1472, 1256, 1106, 844. ^{1}H-NMR (500 MHz, $CDCl_3$): 0.16 (*s*, 12 H); 0.17 (*s*, 12 H); 0.23 (*s*, 18 H); 0.94 (*s*, 18 H); 0.95 (*s*, 18 H); 4.73 (*s*, 4 H); 4.76 (*s*, 4 H); 7.54 (*m*, *AA′BB′*, 4 H); 8.60 (*m*, *AA′BB′*, 4 H). ^{13}C-NMR (125.8 MHz, $CDCl_3$): −5.05; −5.00; −0.13; 18.54; 25.98; 26.07; 64.46; 64.67; 98.77; 100.03; 102.17; 107.61; 118.86; 126.93; 127.38; 129.57; 131.02; 132.14. FAB-MS: 1046.6 (100, M^+). HR-FAB-MS: 1046.5268 (M^+, $^{12}C_{60}H_{94}O_4{}^{28}Si_6{}^+$; calc. 1046.5767).

*1,4-Bis[(*E*)-3,4-bis[[(*tert*-*butyl*)dimethylsilyloxy]methyl]-6-(trimethylsilyl)hex-3-ene-1,5-diynyl]-2,3,5,6-tetrafluorobenzene* (**8**). A degassed soln. of **15** (0.10 g, 0.23 mmol), 1,4-diiodo-2,3,5,6-tetrafluorobenzene (0.047 g, 0.12 mmol), $[PdCl_2(PPh_3)_2]$ (0.005 g, 0.007 mmol), and CuI (0.003 g, 0.014 mmol) in Et_3N (15 ml) was stirred at r.t. under Ar for 22 h. Workup and purification by CC (SiO_2-*60*; hexane/PhMe 1 : 2) afforded **8** (0.035 g, 33%). Yellow solid. M.p. 125–126°. UV/VIS ($CHCl_3$): 340 (sh, 47000), 359 (67700), 382 (57400). IR ($CHCl_3$): 2996, 2856, 2200, 2133, 1489, 1256, 1222, 1106, 983, 844, 789. ^{1}H-NMR (300 MHz, $CDCl_3$): 0.085 (*s*, 12 H); 0.090 (*s*, 12 H); 0.20 (*s*, 18 H); 0.898 (*s*, 18 H); 0.902 (*s*, 18 H); 4.50 (*s*, 4 H); 4.53 (*s*, 4 H). ^{13}C-NMR (75.5 MHz, $CDCl_3$): −5.46; −5.43; −0.36; 18.29; 25.77; 63.64; 63.72; 80.38; 100.39; 101.30; 109.15; 129.06; 133.12; 144.61; 148.20. ^{19}F-NMR (282 MHz, $CDCl_3$): −136.60. FAB-MS: 1019.4 (23, MH^+), 961.3 (100, $[M-Me_3C]^+$). Anal. calc. for $C_{52}H_{86}F_4O_4Si_6$ (1019.76): C 61.25, H 8.50; found: C 61.34, H 8.71.

*1,4-Bis[(*E*)-3,4-bis[[(*tert*-*butyl*)dimethylsilyloxy]methyl]-6-(trimethylsilyl)hex-3-ene-1,5-diynyl]-2,3,5,6-tetramethylbenzene* (**9**). A degassed soln. of **15** (0.10 g, 0.23 mmol), 1,4-diiodo-2,3,5,6-tetramethylbenzene (0.044 g, 0.11 mmol, *ca.* 90% purity), $[PdCl_2(PPh_3)_2]$ (0.005 g, 0.007 mmol), and CuI (0.003 g, 0.016 mmol) in Et_3N (4 ml) and PhMe (10 ml) was stirred at 70° under Ar for 18 h. Workup and purification by CC (SiO_2-*60*; hexane/PhMe 1 : 1) furnished **9** (0.012 g, 12%). Yellow solid. M.p. 137–138°. UV/VIS ($CHCl_3$): 253 (19700), 286 (sh, 10500), 307 (14800), 344 (sh, 36800), 361 (49200), 384 (40100). IR ($CHCl_3$): 3000, 2956, 2936, 2856, 2133, 1600, 1472, 1250, 1183, 1100, 1039, 1006, 933, 844. ^{1}H-NMR (500 MHz, $CDCl_3$): 0.0855 (*s*, 12 H); 0.0863 (*s*, 12 H); 0.20 (*s*, 18 H); 0.89 (*s*, 18 H); 0.90 (*s*, 18 H); 2.40 (*s*, 12 H); 4.53 (*s*, 4 H); 4.57 (*s*, 4 H). ^{13}C-NMR (125.8 MHz, $CDCl_3$): −5.40; −5.36; −0.39; 18.20; 25.66; 25.76; 63.86; 64.37; 95.38; 100.38; 101.83; 106.28; 123.46; 128.73; 130.59; 135.56. FAB-MS: 1003.5 (75, MH^+), 945.4 (100, $[M-Me_3C]^+$). HR-FAB-MS: 1002.6098 (M^+, $^{12}C_{56}H_{98}O_4{}^{28}Si_6{}^+$; calc. 1002.6080).

*2,5-Bis[(*E*)-3,4-bis[[(*tert*-*butyl*)dimethylsilyloxy]methyl]-6-(trimethylsilyl)hex-3-ene-1,5-diynyl]pyridine* (**10**). A degassed soln. of **15** (0.10 g, 0.23 mmol), 2,5-dibromopyridine (0.027 g, 0.11 mmol), $[PdCl_2(PPh_3)_2]$ (0.005 g, 0.007 mmol), and CuI (0.003 g, 0.016 mmol) in Et_3N (20 ml) was stirred at 80° under Ar for 18 h. Workup and purification by CC (SiO_2-*60*; hexane/PhMe 3 : 2 + 1% Et_3N) gave **10** (0.074 g, 71%). Pale-yellow solid. M.p. 61–62°. UV/VIS ($CHCl_3$): 298 (sh, 35100), 321 (48400), 337 (46800), 376 (sh, 10200). IR ($CHCl_3$): 3000, 2956, 2936, 2856, 2200, 2133, 1473, 1461, 1361, 1250, 1100, 1006, 939, 839. ^{1}H-NMR (300 MHz, $CDCl_3$): 0.079 (*s*, 12 H); 0.087 (*s*, 12 H); 0.19 (*s*, 18 H); 0.89 (*s*, 36 H); 4.49 (*s*, 4 H); 4.53 (*s*, 4 H); 7.28 (*d*, *J* = 8.1, 1 H); 7.76 (*dd*, *J* = 8.1, 2.7, 1 H); 8.63 (*d*, *J* = 2.7, 1 H). ^{13}C-NMR (75.5 MHz, $CDCl_3$): −5.72; −5.69; −0.80; 17.84; 25.36; 63.44; 63.49; 87.00; 98.57; 101.15; 107.58; 119.74; 126.18; 127.77; 129.14; 131.47; 138.38; 141.37; 150.98. FAB-MS: 948.5 (100, MH^+). HR-FAB-MS: 948.5510 (MH^+, $^{12}C_{51}H_{90}NO_4{}^{28}Si_6{}^+$; calc. 948.5485).

*2,5-Bis[(*E*)-3,4-bis[[(*tert*-*butyl*)dimethylsilyloxy]methyl]-6-(trimethylsilyl)hex-3-ene-1,5-diynyl]pyrazine* (**11**). A degassed soln. of **15** (0.145 g, 0.33 mmol), 2,5-dibromopyrazine (0.039 g, 0.17 mmol), $[PdCl_2(PPh_3)_2]$ (0.007 g, 0.010 mmol), and CuI (0.004 g, 0.020 mmol) in Et_3N (5 ml) and PhMe (10 ml) was stirred at 80° under Ar for 18 h. Workup and purification by CC (SiO_2-*60*; hexane/AcOEt 15 : 1) afforded **11** (0.129 g, 82%). Pale yellow solid. M.p. 56–58°. UV/VIS ($CHCl_3$): 286 (18700), 307 (20200), 375 (50600), 392 (sh, 41900). IR ($CHCl_3$): 3022, 2956, 2953, 2856, 2133, 1472, 1470, 1255, 1207, 1100, 844, 817. ^{1}H-NMR (500 MHz, $CDCl_3$): 0.092 (*s*, 12 H); 0.099 (*s*, 12 H); 0.20 (*s*, 18 H); 0.90 (*s*, 36 H); 4.50 (*s*, 4 H); 4.54 (*s*, 4 H); 8.58 (*s*, 2 H). ^{13}C-NMR (125.8 MHz, $CDCl_3$): −5.39; −5.35; −0.49; 18.12; 25.64; 63.61; 63.68; 91.80; 97.02; 101.20; 108.65; 128.90; 132.60; 137.47; 146.92. FAB-MS: 949.6 (17, MH^+), 891.5 (100, $[M-Me_3C]^+$). HR-FAB-MS: 948.5327 (M^+, $^{12}C_{50}H_{88}N_2O_4{}^{28}Si_6{}^+$; calc. 948.5359). Anal. calc. for $C_{50}H_{88}N_2O_4Si_6 \cdot 1/2H_2O$ (958.79): C 62.64, H 9.36, N 2.92; found: C 62.51, H 9.17, N 2.88.

*2,5-Bis[(*E*)-3,4-bis[[(*tert*-*butyl*)dimethylsilyloxy]methyl]-6-(trimethylsilyl)hex-3-ene-1,5-diynyl]thiophene* (**12**). A degassed soln. of **15** (0.10 g, 0.23 mmol), 2,5-diiodothiophene (0.038 g, 0.11 mmol), $[PdCl_2(PPh_3)_2]$ (0.005 g, 0.007 mmol), and CuI (0.003 g, 0.016 mmol) in Et_3N (2 ml) and PhMe (10 ml) was stirred at 60° under

Ar for 18 h. Workup and purification by CC (SiO_2-*60*; hexane/PhMe 1:1) yielded **12** (0.055 g, 52%) as a pale yellow oil which eventually crystallized. M.p. 45°. UV/VIS ($CHCl_3$): 260 (19100), 286 (13600), 313 (13600), 367 (sh, 38800), 381 (45900), 404 (sh, 32400). IR ($CHCl_3$): 3011, 2956, 2936, 2856, 2133, 1472, 1261, 1183, 1100, 911, 844. ^{1}H-NMR (200 MHz, $CDCl_3$): 0.10 (*s*, 24 H); 0.20 (*s*, 18 H); 0.910 (*s*, 18 H); 0.914 (*s*, 18 H); 4.45 (*s*, 4 H); 4.51 (*s*, 4 H); 7.05 (*s*, 2 H). ^{13}C-NMR (50 MHz, $CDCl_3$): – 5.91; – 0.93; 17.64; 25.20; 63.16; 63.29; 91.41; 93.22; 101.19; 107.06; 124.45; 129.09; 129.76; 131.31. FAB-MS: 953.2 (52, MH^+), 895.2 (100, $[M - Me_3C]^+$). Anal. calc. for $C_{50}H_{88}O_4Si_6S$ (953.83): C 62.96, H 9.30, S 3.36; found: C 63.02, H 9.53, S 3.15.

*2,5-Bis[(*E*)-3,4-bis[[(*tert*-butyl)dimethylsilyloxy]methyl]-6-(trimethylsilyl)hex-3-ene-1,5-diynyl]furan* (**13**). A degassed soln. of **15** (0.120 g, 0.27 mmol), 2,5-dibromofuran (0.031 g, 0.14 mmol, *ca.* 90% purity), $[PdCl_2(PPh_3)_2]$ (0.006 g, 0.009 mmol), and CuI (0.003 g, 0.016 mmol) in Et_3N (4 ml) and PhMe (10 ml) was stirred at 70° under Ar for 48 h. Workup and purification by CC (SiO_2-*60*; hexane/PhMe 1:2) furnished **13** (0.035 g, 30%). Colorless oil. UV/VIS ($CHCl_3$): 255 (11900), 291 (14500), 304 (17200), 358 (sh, 26900), 372 (32200), 398 (sh, 23900). IR ($CHCl_3$): 3000, 2956, 2936, 2856, 2133, 1472, 1463, 1250, 1139, 1100, 844. ^{1}H-NMR (500 MHz, $CDCl_3$): 0.090 (*s*, 12 H); 0.091 (*s*, 12 H); 0.19 (*s*, 18 H); 0.900 (*s*, 18 H); 0.906 (*s*, 18 H); 4.44 (*s*, 4 H); 4.50 (*s*, 4 H); 6.57 (*s*, 2 H). ^{13}C-NMR (125.8 MHz, $CDCl_3$): – 5.42; – 5.36; – 0.45; 18.14; 25.647; 25.654; 63.55; 63.60; 90.49; 91.55; 101.43; 107.65; 116.82; 129.34; 130.07; 137.57. FAB-MS: 937.8 (36, MH^+), 879.7 (100, $[M - Me_3C]^+$). HR-FAB-MS: 936.5265 (M^+, $^{12}C_{50}H_{88}O_5{}^{28}Si_6{}^+$; calc. 936.5247).

trans-*Bis[(*E*)-3,4-bis[[(*tert*-butyl)dimethylsilyloxy]methyl]-6-(trimethylsilyl)hex-3-ene-1,5-diynyl]bis(triethylphosphine)platinum(II)* (**14**). To a degassed soln. of **15** (0.10 g, 0.23 mmol) and *trans*-$[PtCl_2(PEt_3)_2]$ (0.057 g, 0.11 mmol) in anh. THF (2 ml) and $(i\text{-}Pr)_2NH$ (0.5 ml) was added CuI (0.001 g, 0.006 mmol). Within minutes, a white solid precipitated. The mixture was stirred at r.t. under N_2 for 20 h. Workup and purification by CC (SiO_2-*60*; hexane) and prep. TLC (SiO_2; hexane/CH_2Cl_2 4:1) afforded **14** (0.097 g, 65%). Pale yellow solid. M.p. 102°. UV/VIS ($CHCl_3$): 227 (sh, 19300), 303 (34200), 332 (41300), 342 (42300). IR ($CHCl_3$): 2959, 2856, 2133, 2068, 1471, 1462, 1251, 1095, 1036, 844. ^{1}H-NMR (200 MHz, $CDCl_3$): 0.06 (*s*, 12 H); 0.07 (*s*, 12 H); 0.16 (*s*, 18 H); 0.88 (*s*, 18 H); 0.89 (*s*, 18 H); 1.09 (*quint.*, $J = 7.8$ Hz, 18 H); 1.95 – 2.08 (*m*, 12 H); 4.39 (*s*, 4 H); 4.46 (*s*, 4 H). ^{13}C-NMR (50 MHz, $CDCl_3$): – 5.15; – 5.05; – 0.04; 8.22 (*t*, J(P,C) = 13); 16.18 (*quint.*, J(P,C) = 18); 18.41; 25.93; 26.05; 64.08; 65.73; 103.06; 104.14; 108.08; 123.34; 124.39 (*t*, J(P,C) = 13); 135.02 (*t*, J(P,C) = 8). ^{31}P-NMR (121.5 MHz, $CDCl_3$): 12.41 (*t*, J(P,Pt) = 2936). FAB-MS: 1301.4 (M^+). Anal. calc. for $C_{58}H_{116}O_4P_2PtSi_6 \cdot H_2O$ (1321.13): C 52.73, H 9.00; found: C 52.86, H 8.73.

This work was supported by a grant from the *ETH Research Council*. We thank Dipl. Chem. *Michael Edelmann* for assistance in the determination of fluorescence quantum yields.

REFERENCES

[1] A. Rajca, *Chem. Rev.* **1994**, *94*, 871; J. S. Miller, A. J. Epstein, *Angew. Chem.* **1994**, *106*, 399; *ibid., Int. Ed.* **1994**, *33*, 385; J. S. Miller, *Adv. Mater.* **1992**, *4*, 435.

[2] 'Handbook of Conducting Polymers', Eds. T. A. Skotheim, R. L. Elsenbaumer, J. R. Reynolds, Marcel Dekker, New York, 1998; 'Handbook of Organic Conductive Molecules and Polymers', Ed. H. S. Nalwa, J. Wiley & Sons, Chichester, Vols. 1 – 4, 1997.

[3] R. H. Friend, R. W. Gymer, A. B. Holmes, J. H. Burroughes, R. N. Marks, C. Taliani, D. D. C. Bradley, D. A. Dos Santos, J. L. Brédas, M. Lögdlund, W. R. Salaneck, *Nature (London)* **1999**, *397*, 121; A. Kraft, A. C. Grimsdale, A. B. Holmes, *Angew. Chem.* **1998**, *110*, 416; *ibid., Int. Ed.* **1998**, *37*, 402; J. L. Segura, *Acta Polym.* **1998**, *49*, 319.

[4] G. Horowitz, *Adv. Mater.* **1998**, *10*, 365; H. E. Katz, J. G. Laquindanum, A. J. Lovinger, *Chem. Mater.* **1998**, *10*, 633; T. Siegrist, C. Kloc, R. A. Laudise, H. E. Katz, R. C. Haddon, *Adv. Mater.* **1998**, *10*, 379; G. Barbarella, P. Ostoja, P. Maccagnani, O. Pudova, L. Antolini, D. Casarini, A. Bongini, *Chem. Mater.* **1998**, *10*, 3683; H. Sirringhaus, R. H. Friend, X. C. Li, S. C. Moratti, A. B. Holmes, N. Feeder, *Appl. Phys. Lett.* **1997**, *71*, 3871; R. Hajlaoui, D. Fichou, G. Horowitz, B. Nessakh, M. Constant, F. Garnier, *Adv. Mater.* **1997**, *9*, 557; D. Fichou, M.-P. Teulade-Fichou, G. Horowitz, F. Demanze, *Adv. Mater.* **1997**, *9*, 75.

[5] A. J. Heeger, J. Long, Jr., *Optics & Photonics News* **1996**, *7*, 24; H. S. Nalwa, in 'Nonlinear Optics of Organic Molecules and Polymers', Eds. H. S. Nalwa, S. Miyata, CRC Press, New York, 1997, pp. 611 – 798; S. R. Marder, B. Kippelen, A. K.-Y. Jen, N. Peyghambarian, *Nature (London)* **1997**, *388*, 845; R. R. Tykwinski, U. Gubler, R. E. Martin, F. Diederich, C. Bosshard, P. Günter, *J. Phys. Chem. B* **1998**, *102*, 4451.

[6] R. E. Martin, U. Gubler, C. Boudon, V. Gramlich, C. Bosshard, J.-P. Gisselbrecht, P. Günter, M. Gross, F. Diederich, *Chem. Eur. J.* **1997**, *3*, 1505.

[7] R. E. Martin, T. Mäder, F. Diederich, *Angew. Chem.* **1999**, *111*, 834; *ibid., Int. Ed.* **1999**, *38*, 817.
[8] R. E. Martin, Dissertation, ETH-Zürich, Diss. ETH No. 12821, Zürich, 1998.
[9] M. Schreiber, J. Anthony, F. Diederich, M. E. Spahr, R. Nesper, M. Hubrich, F. Bommeli, L. Degiorgi, P. Wachter, P. Kaatz, C. Bosshard, P. Günter, M. Colussi, U. W. Suter, C. Boudon, J.-P. Gisselbrecht, M. Gross, *Adv. Mater.* **1994**, *6*, 786.
[10] M. Schreiber, Dissertation, ETH-Zürich, Diss. ETH No. 11904, Zürich, 1996.
[11] C. Bosshard, R. Spreiter, P. Günter, R. R. Tykwinski, M. Schreiber, F. Diederich, *Adv. Mater.* **1996**, *8*, 231.
[12] M. Schreiber, R. R. Tykwinski, F. Diederich, R. Spreiter, U. Gubler, C. Bosshard, I. Poberaj, P. Günter, C. Boudon, J.-P. Gisselbrecht, M. Gross, U. Jonas, H. Ringsdorf, *Adv. Mater.* **1997**, *9*, 339.
[13] C. Dehu, F. Meyers, J. L. Brédas, *J. Am. Chem. Soc.* **1993**, *115*, 6198.
[14] J. Zyss, in 'Conjugated Polymeric Materials: Opportunities in Electronics, Optoelectronics, and Molecular Electronics', Eds.: J. L. Brédas, R. R. Chance, NATO ASI Ser, Ser. E., Vol. 182, Kluwer Academic Publishers, Dordrecht, 1990, pp. 545–557.
[15] C. R. Moylan, R. D. Miller, R. J. Twieg, K. M. Betterton, V. Y. Lee, T. J. Matray, C. Nguyen, *Chem. Mater.* **1993**, *5*, 1499.
[16] R. Faust, F. Diederich, V. Gramlich, P. Seiler, *Chem. Eur. J.* **1995**, *1*, 111.
[17] J. Wytko, V. Berl, M. McLaughlin, R. R. Tykwinski, M. Schreiber, F. Diederich, C. Boudon, J.-P. Gisselbrecht, M. Gross, *Helv. Chim. Acta* **1998**, *81*, 1964.
[18] R. E. Martin, F. Diederich, *Angew. Chem.* **1999**, *111*, 1440; *ibid., Int. Ed.* **1999**, *38*, 1350.
[19] S. Takahashi, Y. Kuroyama, K. Sonogashira, N. Hagihara, *Synthesis* **1980**, 627; K. Sonogashira, in 'Metal-catalyzed Cross-coupling Reactions', Eds. F. Diederich, P. J. Stang, Wiley-VCH, Weinheim, 1987, pp. 203–229.
[20] R. R. Tykwinski, M. Schreiber, R. Pérez Carlón, F. Diederich, V. Gramlich, *Helv. Chim. Acta* **1996**, *79*, 2249.
[21] D. A. de Bie, A. Ostrowicz, G. Geurtsen, H. C. van der Plas, *Tetrahedron* **1988**, *44*, 2977.
[22] R. C. Ellingson, R. L. Henry, *J. Am. Chem. Soc.* **1949**, *71*, 2798.
[23] M. Takeuchi, T. Tuihiji, J. Nishimura, *J. Org. Chem.* **1993**, *58*, 7388.
[24] Z. Bao, W. K. Chan, L. Yu, *J. Am. Chem. Soc.* **1995**, *117*, 12426; R. Singh, G. Just, *J. Org. Chem.* **1989**, *54*, 4453.
[25] V. Grosshenny, F. M. Romero, R. Ziessel, *J. Org. Chem.* **1997**, *62*, 1491.
[26] K. Sonogashira, Y. Fujikura, T. Yatake, N. Toyoshima, S. Takahashi, N. Hagihara, *J. Organomet. Chem.* **1978**, *145*, 101.
[27] M. J. Church, M. J. Mays, *J. Chem. Soc. A* **1968**, 3074; E. W. Randall, D. Shaw, *Mol. Phys.* **1965**, *10*, 41.
[28] P. Siemsen, P. Seiler, F. Diederich, to be published.
[29] G. G. Guilbault, in 'Practical Fluorescence', Ed. G. G. Guilbault, Marcel Dekker, New York, 1990, pp. 1–40.
[30] 'Sadtler Standard Ultraviolet Spectra', Vol. 2, Sadtler Research Laboratories, Philadelphia, 1972, Spectrum 394.
[31] V. Grosshenny, A. Harriman, M. Hissler, R. Ziessel, *J. Chem. Soc., Faraday Trans.* **1996**, *92*, 2223.
[32] I. D. L. Albert, T. J. Marks, M. A. Ratner, *J. Am. Chem. Soc.* **1997**, *119*, 6575.
[33] V. I. Minkin, M. N. Glukhovtsev, B. Y. Simkin, 'Aromaticity and Antiaromaticity. Electronic and Structural Aspects', Wiley, New York, 1994, Chapt. 5, pp. 217–229.
[34] L. Gobbi, P. Seiler, F. Diederich, *Angew. Chem.* **1999**, *111*, 740; *ibid., Int. Ed.* **1999**, *38*, 674.
[35] V. Balzani, M. Gómez-López, J. F. Stoddart, *Acc. Chem. Res.* **1998**, *31*, 405; A. P. de Silva, H. Q. N. Gunaratne, T. Gunnlaugsson, A. J. M. Huxley, C. P. McCoy, J. T. Rademacher, T. E. Rice, *Chem. Rev.* **1997**, *97*, 1515; P. A. Ashton, R. Ballardini, V. Balzani, M. Gómez-López, S. E. Lawrence, M. V. Martínez-Díaz, M. Montalti, A. Piersanti, L. Prodi, J. F. Stoddart, D. J. Williams, *J. Am. Chem. Soc.* **1997**, *119*, 10641; V. Balzani, F. Scandola, in 'Comprehensive Supramolecular Chemistry', Ed. D. N. Reinhoudt, Pergamon Press, Oxford, 1996, Vol. 10, pp. 687–746; B. L. Feringa, W. F. Jager, B. de Lange, *Tetrahedron* **1993**, *49*, 8267.
[36] D. D. Gebler, Y. Z. Wang, D.-K. Fu, T. M. Swager, A. J. Epstein, *J. Chem. Phys.* **1998**, *108*, 7842; M. Fahlman, D. D. Gebler, N. Piskun, T. M. Swager, A. J. Epstein, *J. Chem. Phys.* **1998**, *109*, 2031; J. W. Blatchford, T. L. Gustafson, A. J. Epstein, *J. Chem. Phys.* **1996**, *105*, 9214.
[37] D. A. Skoog, 'Principles of Instrumental Analysis', CBS College Publishing, Philadelphia, 1985, p. 232.
[38] A. M. Bond, R. Colton, D. A. Fiedler, J. E. Kevekordes, V. Tedesco, T. F. Mann, *Inorg. Chem.* **1994**, *33*, 5761; S. Hasenzahl, H.-D. Hausen, W. Kaim, *Chem. Eur. J.* **1995**, *1*, 95.
[39] D. R. Liu, P. G. Schultz, *Angew. Chem.* **1999**, *111*, 36; *ibid., Int. Ed.* **1999**, *38*, 36.

Received June 15, 1999